# Influence of metal-oxide interfaces on L1(2) ordering in CU3Pd

Mogck, S.; Kooi, B.J.; de Hosson, J.T.M.

*Published in:*
Acta Materialia

*DOI:*
10.1016/j.actamat.2004.06.021



*Publication date:*
2004

Available online at www.sciencedirect.com
SCIENCE DIRECT®
Acta Materialia 52 (2004) 4651–4658
Acta MATERIALIA
www.actamat-journals.com

# Influence of metal–oxide interfaces on $L1_2$ ordering in $Cu_3Pd$

S. Mogck, B.J. Kooi, J.Th.M. De Hosson *

*Department of Applied Physics, Materials Science Center and the Netherlands Institute of Metals Research, University of Groningen, Nijenborgh 4, 9747 AG Groningen, The Netherlands*

Received 16 April 2004; received in revised form 2 June 2004; accepted 11 June 2004
Available online 15 July 2004

**Abstract**

A strong influence of the polarity on the degree of $L1_2$ order near interfaces between $Cu_3Pd$ and MnO has been observed. In situ TEM annealing at various temperatures was performed to re-establish the $L1_2$ ordering in $Cu_3Pd$ alloy containing MnO precipitates. Subsequently, high-resolution transmission electron microscopy was used to analyze the long-range order in $Cu_3Pd$ ($L1_2$) at parallel {0 0 2} and parallel {1 1 1} $Cu_3Pd$–MnO interfaces. Analyses of the polar {1 1 1} interfaces in the ⟨1 1 0⟩ and ⟨1 1 2⟩ projection show a gradual disappearance of $L1_2$ order within the $Cu_3Pd$ with decreasing distance to these interfaces. The interesting point is that the $L1_2$ order dissolves over about 10 monolayers (MLs). In contrast, for the non-polar parallel {0 0 2} interface viewed along ⟨1 0 0⟩ no influence on the $L1_2$ order and APB structure, even close to the interface could be observed. Analytical TEM analysis revealed a small enrichment of Pd at the {1 1 1} $Cu_3Pd$–MnO interface in the $Cu_3Pd$ ML nearest to the interface. This phenomenon is not considered responsible for the interfacial disorder extending over such a large length scale. Physical effects that cause the disordering at the polar interface are discussed. The conclusion of the analysis is that the dipolar contribution to the internal energy acts as an initiation of disordering along the MnO/$Cu_3Pd$ interface but that the configurational entropy determines the extension of the disordered area.


*Keywords:* Interfaces; High-resolution electron microscopy; Intermetallic compounds; Oxides; Ordering

## 1. Introduction

Ordered alloys have been a topic of considerable interest over the last decades because of their potential use in high-temperature applications [1]. The transition temperature of chemical long-range order to disorder depends on the precise chemical composition of the intermetallic compounds. In this work we concentrate only on long-range order and not on short-range order that may exist even above the transition temperature. Also well established in $L1_2$ ordered structures are so-called long period superstructures (LPS), i.e. equilibrium structures with an ordered array of parallel anti-phase boundaries (APBs) with a particular periodic distance. In the binary Cu–Pd system the $L1_0$ ordering but also $L1_2$ ordering for the Cu-rich compound and one and two-dimensional LPS in $L1_2$ have been observed [2]. The LPS was detected between 17 and 30 at.% Pd and LPS was studied as a function of temperature by Broddin et al. [2]. A more detailed analysis of the composition range between 18 and 21 at.% Pd was carried out to study chaotic and uniform regimes in incommensurate APBs [3]. The transition from the $L1_2$ structure at low temperature to the LPS at higher temperatures have been studied and the LPS retains up to the order/disorder transition temperature (Guymont and Gratias) [4]. Near this transition temperature ($T_c$) the APBs become wetted by the disordered phase and the thickness of this wetting layer scales with $\log(T - T_c)^{-1}$, so that only starting from about 1 K below and up to $T_c$ substantial wetting is detected.

In the present work, high-resolution transmission electron microscopy (HRTEM) is used to study in detail the $L1_2$ order in $Cu_3Pd$ near its interface with MnO. In situ heating is used to re-establish the order that was

* Corresponding author. Tel.: +31-503-634-898; fax: +31-503-634-881.
*E-mail address:* hossonj@phys.rug.nl (J.T.M. De Hosson).

1359-6454/$30.00 © 2004 Published by Elsevier Ltd on behalf of Acta Materialia Inc.
doi:10.1016/j.actamat.2004.06.021

slightly damaged by the sample preparation. HRTEM images were taken from edge-on non-polar parallel {0 0 2} interfaces as viewed along ⟨1 0 0⟩ and from edge-on polar parallel {1 1 1} $Cu_3Pd$–MnO interfaces as viewed along both ⟨1 1 0⟩ and ⟨1 1 2⟩.

## 2. Experimental

A $Cu_3Pd$ alloy containing 1.5 at.% Mn was prepared by melting the elements (purity 99.99 wt%) together in an arc furnace. The ingot was homogenized (1 week 700 °C) and subsequently cold rolled to foils of an approximate thickness of 250 μm. Internal oxidation was performed using the so-called Rhines pack technique [5] at 900 °C for 17 h in an evacuated quartz tube. The internally oxidized alloy was annealed at 450 °C for 24 h in vacuo and subsequently quenched in direct contact with water. Discs were punched out of the foils for TEM observations.

Thinning of the discs was performed by electro-polishing using an electrolyte containing 78% $CH_3OH$ and 22% $HNO_3$. Voltages in the range of 15–20 V were applied. After electropolishing the discs of the internally oxidized alloy were covered with a thin oxide layer (a problem that does not occur for the pure metallic Cu–Pd system). Ion milling (Gatan PIPS model 691) was used to remove these thin oxide layers and to further reduce the thickness of the oxide precipitates. The time for ion milling was kept shorter than 30 min at 2.5 kV avoiding damage of the $L1_2$ ordering as much as possible and disappearance of the ordered APB structures in the $Cu_3Pd$ matrix. Merely ion milling as a thinning method was not successful in the preparation of a suitable $Cu_3Pd$ specimen. Even after long in situ annealing in the TEM the LPS could not retrieved. This has been also mentioned in [6].

To re-establish the order and to study the development or disappearance of ordering and LPS as a function of temperature, in situ heating experiments in a TEM were performed. These experiments were carried out in a JEOL 2010F equipped with a Gatan double tilt specimen heating-holder, model 652. The temperature of the heating element is controlled with an accuracy of $\leqslant 1$ °C. During the heating experiments the development of the $L1_2$ ordering in $Cu_3Pd$ and LPS (due to the formation of ordered arrays of APBs) in a temperature range between 450 and 500 °C was carefully monitored.

For HRTEM a JEOL 4000 EX II, operating at 400 kV (spherical aberration coefficient: $0.97 \leqslant 0.02$ mm, defocus spread $7.8 \leqslant 1.4$ nm, beam semi-convergence angle 0.8 mrad) and the Stuttgart JEOL ARM 1250, operating at 1250 kV (spherical aberration coefficient: 2.7 mm, defocus spread 11 nm, beam semi-convergence angle 0.9 mrad) was used. The XEDS measurements were carried out using the JEOL 2010F, operating at 200 kV and equipped with an EDAX X-ray energy-dispersive spectrometer with a super-ultra thin window. For the detection of the composition profile around an edge-on oriented parallel {1 1 1} $Cu_3Pd$–MnO planar interface an electron probe diameter of 0.7 nm (FWHM) was used. A detailed description of the method employed to determine the composition profile and the segregation towards heterophase interfaces can be found elsewhere [7–9].

## 3. Results

After the internal oxidation process MnO (NaCl structure) and $Mn_3O_4$ (tetragonal distorted spinel, I4/amd) precipitates in the $Cu_3Pd$ matrix of 100–200 nm [10] were observed. The MnO precipitates are bound by {1 1 1} planes. Additionally the $Mn_3O_4$ precipitates have a small fraction of plate-shaped precipitates with a dominant (0 0 2) facet oriented parallel to {0 0 2} of the $Cu_3Pd$ matrix. The fraction of $Mn_3O_4$ precipitates can be increased by increasing the Mn content in the $Cu_3Pd$ matrix [10] (before oxidation).

All HRTEM observations with the JEOL 4000 EX/II were carried out after the sample was heated in situ in a JEOL 2010F at 480 °C for 1 h and subsequently cooled down by switching off the heating device. Although the sample is in vacuum the cooling in the thin areas of interest for TEM occurs very fast due to the very limited specimen thickness (order of 20 nm). In contrast to the JEOL 4000 EX/II, direct in situ HRTEM observation at 480 °C with the JEOL ARM 1250 could be performed. The temperature of 480 °C, according to the temperature control of the heating device, is 10 °C below the order disorder transition temperature $T_c$ of 490 °C. The HRTEM micrograph depicted in Fig. 1 shows an edge-on parallel {0 0 2} $Cu_3Pd$–$Mn_3O_4$ interface in the ⟨1 0 0⟩ viewing direction as imaged at 480 °C. Note that due to the in situ heating the $Mn_3O_4$ has been reduced to MnO. In the following $Mn_3O_4$ will be mentioned to refer to the starting structure, but is has to be kept in mind that after the in situ heat treatment it is always reduced to MnO. Using the ⟨1 0 0⟩ projection the {0 0 1} APBs are separated by $M = 8 \pm 1$ planes and strike the projected interface perpendicular. It is clearly visible that the $L1_2$ ordering in $Cu_3Pd$ exists up to the interface. Moreover, the APBs oriented perpendicularly the $Cu_3Pd$–MnO interface do not change their behavior upon approaching the interface. Apparently, this parallel {0 0 2} type of interface between $Cu_3Pd$ and $Mn_3O_4$ does not change the structure of the APBs (e.g. deflection or wetting of the APBs) and does not influence the $L1_2$ ordering in the $Cu_3Pd$ matrix at this temperature.

In contrast, the polar {1 1 1} $Cu_3Pd$–MnO interface as shown in Fig. 2 reveals a different degree of the $L1_2$ ordering directly at the interface. In order to determine

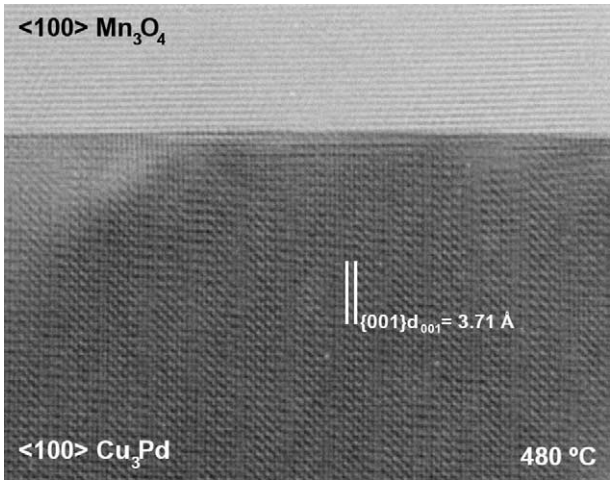


Fig. 1. HRTEM image in the ⟨1 0 0⟩ projection of $Cu_3Pd$–$Mn_3O_4$ interface recorded in situ at 480 °C with the Stuttgart JEOL ARM 1250 transmission electron microscope. The $L1_2$ ordering and the APBs (perpendicular to the interface) persist up to the interface. Due to the heating at 480 °C in the TEM the $Mn_3O_4$ precipitates start to reduce to MnO.

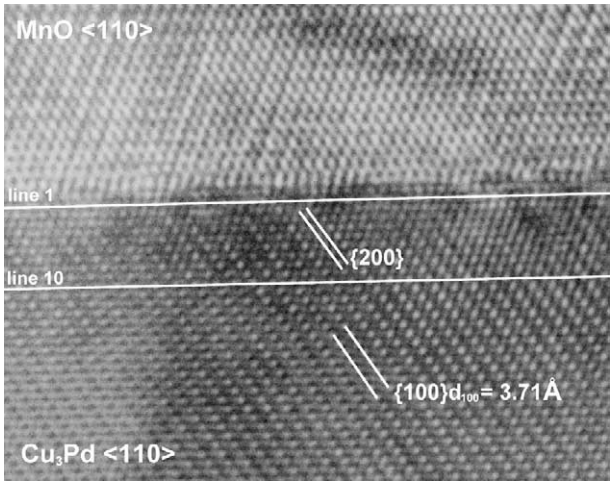


Fig. 2. HRTEM image of a {1 1 1} $Cu_3Pd$–MnO interface in the ⟨1 1 0⟩ viewing direction. The first and the 10th line profile, highlighted by white solid lines along the interface, are Fourier transformed and the result of this procedure is depicted in Fig. 3.

the degree of $L1_2$ order in $Cu_3Pd$ as a function of distance to the parallel {1 1 1} $Cu_3Pd$–MnO interface, line-scans parallel to the interface (⟨1 1 2⟩ direction) with a width of 3 pixels (perpendicular to the interface) were taken directly on top of the atomic columns. The 8 bit gray scale values of these line profiles were converted with fast fourier transformation (FFT) to extract the first-order super-reflection peak and the second-order base-reflection peak. The ratio of the amplitudes of this first and second order reflections (Fig. 3) will be called for the simplicity the {1 0 0}/{2 0 0} (super-reflection/base-reflection) ratio to analyze the $L1_2$ ordering at {1 1 1}$Cu_3Pd$–MnO interfaces in the ⟨1 1 0⟩ projection as

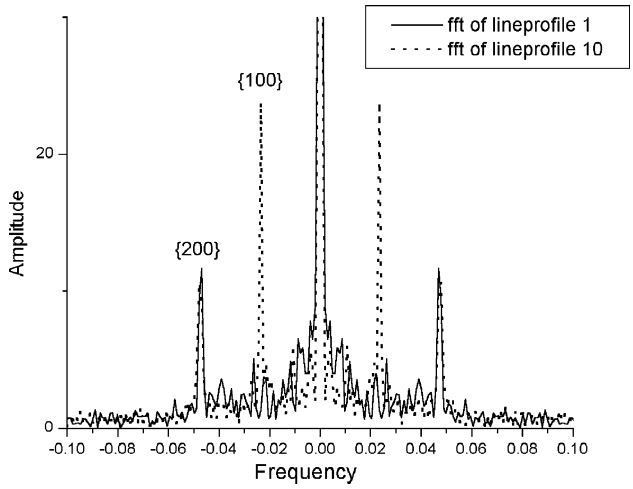


Fig. 3. FFT on line-scans of line 1 and 10, seen in Fig. 2. The peak of the super reflection due to the ordering of $Cu_3Pd$ can be hardly seen in line 1, whereas in line 10 the first-order peak is clearly visible.

a function of distance to the interface. In Fig. 3, the Fast Fourier Transform on a line-scan close to the $Cu_3Pd$–MnO interface (line 1 as indicated in Fig. 2) and a line-scan in the $Cu_3Pd$ matrix (line 10 as indicated in Fig. 2) shows clearly the disappearance of the first order super reflections close to the interface. The {1 0 0}/{2 0 0} ratio (degree of order) as a function of distance to the interface is shown in Fig. 4. This plot indicates that the ordering gradually disappears when approaching the {1 1 1} $Cu_3Pd$–MnO interfaces within a length scale of about 10 monolayers (MLs) for different defoci. Different defoci used for recording the HRTEM images resulted in different {1 0 0}/{2 0 0} ratios in the $Cu_3Pd$ matrix, i.e. at relative large distance to the interface (see Fig. 4). HRTEM image simulations (MacTempas [11])

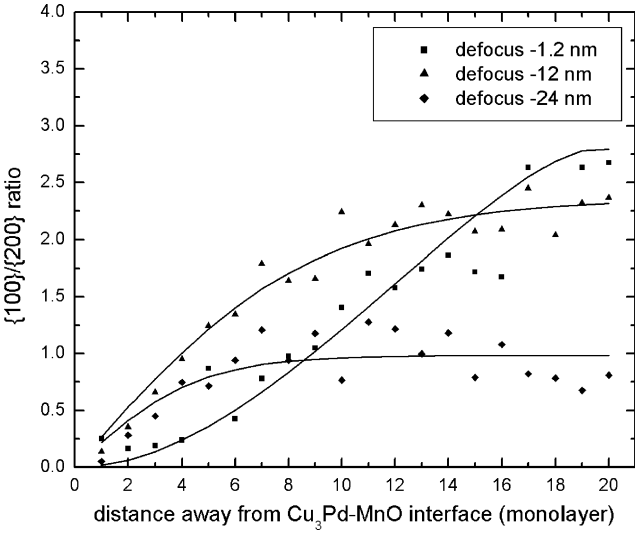


Fig. 4. {1 0 0}/{2 0 0} ratio at 480 °C to visualize degree of $L1_2$ ordering in $Cu_3Pd$ at {1 1 1} $Cu_3Pd$–MnO interfaces for different defoci.

for perfectly ordered $Cu_3Pd$ show that the {1 0 0}/{2 0 0} ratio depends *sensitively* on the TEM specimen thickness and on the defocus used. Despite this strong sensitivity and the large variation that can occur for the {1 0 0}/{2 0 0} ratios it can be concluded that the experimentally obtained ratios are able to confirm the simulated ones (see Table 1).

The TEM samples are in situ heated at 480 °C and this leads to thicker areas under investigation. In order to reduce its relative surface area the specimen retracts the thinnest parts and the wedge shaped specimen becomes blunter. On the other hand, if HRTEM images of $Cu_3Pd$–MnO interfaces with a reasonable atomic resolution are recorded the specimen cannot be too thick (e.g. <20 nm). Therefore, it is not unreasonable that an intermediate thickness of 10–12 nm used in the simulations gives a proper match to the experimental thickness of the HRTEM micrographs. A problem can be that a thickness gradient along the interface occurs, due to the wedge shape of the TEM specimen. We have tried to minimize this effect by using, for the analysis shown in Figs. 3 and 4, interfaces that ran parallel to the edge with the hole in the TEM specimen. Still, because the measured ratio is strongly dependent on thickness, it may cause deviations between the experimentally obtained and simulated {1 0 0}/{2 0 0} ratios. The same of course does not apply only to the ratios measured for bulk $Cu_3Pd$, but for the whole profile as a function of distance to the interface. Particularly, at an interface between dissimilar materials like MnO and $Cu_3Pd$ the presence of thickness variation perpendicular to the interface can hardly be avoided. This may also be the reason why not all the *shapes* of the profiles for the different defoci are identical.

The gradual disappearance of the $L1_2$ ordering in the ⟨1 1 0⟩ projection at polar {1 1 1} $Cu_3Pd$–MnO interfaces can be confirmed also in the ⟨1 1 2⟩ projection, as is illustrated in Fig. 5. Also in this projection the gradual disappearance of the $L1_2$ ordering is demonstrated by performing a line-scan perpendicular to the interface (width of 400 pixels). The result is depicted in Fig. 6. Also in this case the region from order to disorder at the interface appears to occur over about 10 MLs.

Summarizing, the present results clearly indicate that at parallel {0 0 2} $Cu_3Pd$–MnO interfaces disordering does not occur (as observed both at high temperature and after cooling to room temperature), whereas at parallel {1 1 1} $Cu_3Pd$–MnO interfaces disordering does occur as observed using both ⟨1 1 0⟩ and ⟨1 1 2⟩ projections.

Table 1
{1 0 0}/{2 0 0} ratio in the $Cu_3Pd$ matrix of experimental HRTEM images (see Fig. 4) and simulated images of ordered $Cu_3Pd$ for different defoci

| Defocus (nm) | Experiment | Simulation |
|---|---|---|
| 0/−1.2 | 2.91 | 4.27/3.21 |
| −12 | 2.30 | 2.63/1.26 |
| −24 | 0.97 | 4.81/0.58 |

The values listed under simulation correspond to a thickness of 10 nm/12 nm.

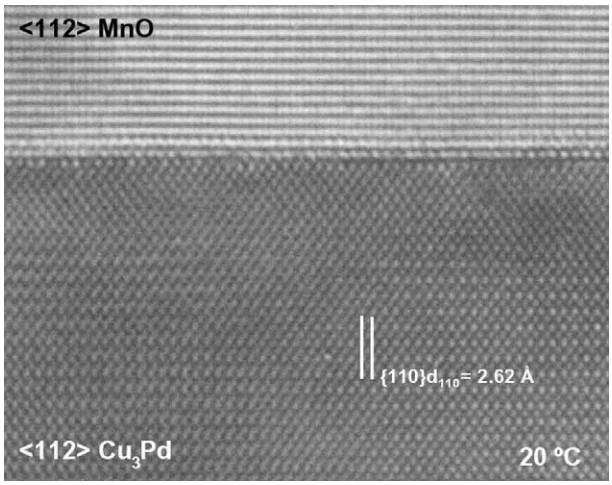


Fig. 5. HRTEM image of a {1 1 1} $Cu_3Pd$–MnO interface in the ⟨1 1 2⟩ viewing direction. The degree of $L1_2$ ordering gradually disappears when approaching the {1 1 1} $Cu_3Pd$–MnO interface.

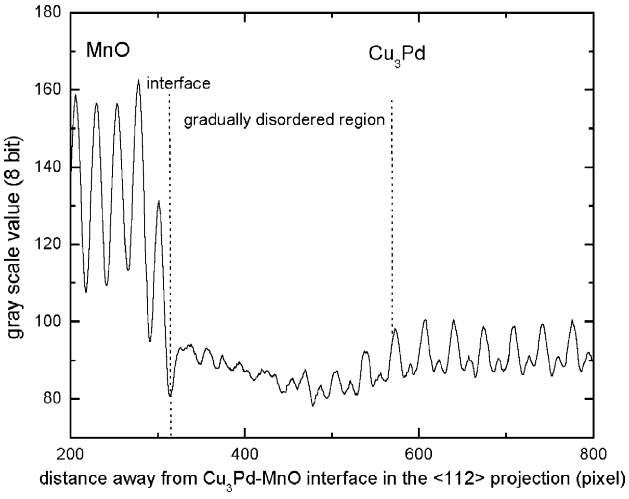


Fig. 6. Line profile with a width of 400 pixel across the $Cu_3Pd$–MnO interface in the ⟨1 1 2⟩ projection shows clearly the disappearance of the $L1_2$ ordering when approaching the interface of about 10 MLs by counting the peaks in the gradually disordered region.

## 4. Discussion

An important question is if the interface causes locally changes in chemical composition in the $Cu_3Pd$ that may explain the presence of disorder. In the previous work [7,8] we presented a new approach to measure and quantify Gibbsian segregation at heterophase interfaces

that has advantages compared to line scans, chemical maps or the use of scan raster. We have applied this approach to the $Cu_3Pd$–MnO interface and the result is shown in Fig. 7. The measured Pd concentration is plotted as a function of the measured Cu concentration (i.e. across the interface) together with the fitted segregation curve. A linear relationship between the Pd and Cu concentrations would indicate that segregation does not occur. The result of the fitting shows a weak Pd segregation at the interface with 26.6 at.% Pd in the metal ML mostly near the interface compared to a measured Pd concentration of 21.5 at.% in the $Cu_3Pd$ matrix (the oxygen content of approx. 2.2 at.% in the $Cu_3Pd$ matrix was included in this quantification). This means that the Pd enrichment in a single ML is about 20%. Comparing these concentrations with the Cu–Pd phase diagram [12] and knowing that for the matrix concentration in situ annealing was performed 10 °C below $T_c$, the higher Pd concentration at the interface then results in a temperature above $T_c$. So it is very well possible that during annealing the ML most near to the interface tends to be disordered. Fast cooling of the TEM specimen does not allow the order to (re-)develop. However, it has to be emphasized that the very local enrichment in one ML at the interface is not considered to be responsible because the $L1_2$ ordering disappears over a much longer length-scale of about 10 MLs.

An important characteristic of the {1 1 1} facet of the MnO (and e.g. all ionic compounds with a rock salt or spinel structure) is that it gives rise to a polar interface, because after internal oxidation the outer atomic layer of the MnO is occupied by negatively charged oxygen ions only [13,14]. Perpendicular to the interface a repeat unit with alternating positive Mn and negative O ions occurs, i.e. establishing an electrical dipolar field. For a free surface (oxide–vacuum interface) such a dipolar field would cause a diverging surface energy and thus would never correspond to a stable surface. The free surface will reconstruct in order to arrive at a finite surface energy. Ab initio calculations on polar {0 0 0 1}-surfaces of ZnO demonstrated that the electronic structure in ZnO is disturbed by the polar free surface of about 16 atomic layers into the bulk [15].

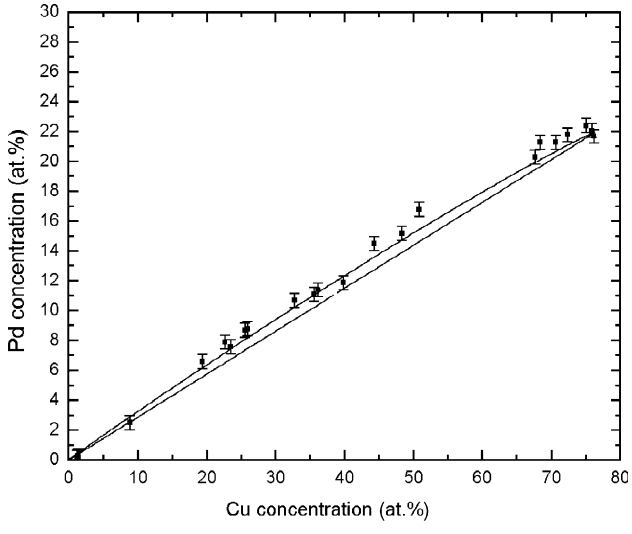


Fig. 7. XEDS results together with the model curve. The best match of the model curve with the XEDS measurement is reached with a Pd concentration of 26.6 at.% in the outermost $Cu_3Pd$ ML at the {1 1 1} $Cu_3Pd$–MnO interface compared with the measured Pd concentration in the $Cu_3Pd$ matrix of 21.9 at.%. A probe size of 1.4 nm was assumed for the fitting procedure between model curve and XEDS data.

For polar oxide–metal interfaces, the situation is essentially different compared with non-polar interfaces: (i) a larger work of adhesion and charge transfer is present (e.g. 0.18e at the parallel {1 1 1} Cu–MgO interface versus 0.08e for the parallel {1 0 0} Cu–MgO interface [16]); (ii) a larger shifts in the layer potentials relative to the bulk is present, and; (iii) a small amplitude electron density oscillation extending at least 5 Å [16] away from the interface into the metal is present for polar interfaces. The metal is very effective in screening the electrical charges in the outer ML of the oxide, but the metal induced gap states (MIGS) in the oxide are supplied by the charges of the bulk metal, rather than the interface layer alone [17,18]. Fluctuating charge density develops along and perpendicular to the interface following the alternating positively and negatively charged layers of the oxide, but with strong damping of these oscillations in electron density in the metal. Ab initio calculations for the polar parallel {1 1 1} Cu/MgO interface confirmed the presence of these charge oscillations in the metal [16], but due to the limited size of the computational cell it was not possible to be conclusive on the range of this interaction.

An important point is that small changes in the interatomic potentials may have a large effect on $T_c$, because, at least in the pair-wise approximation, $T_c$ is more or less a linear function of $w_{ij} = v_{ij} - (v_{ii} + v_{jj})/2$ with $v_{ij}$ the nearest neighbor bond energy between atoms i and j. So, small changes in $v_{Cu–Pd}$, $v_{Cu–Cu}$ or $v_{Pd–Pd}$ may result in a substantial change of $w_{ij}$ that in return clearly changes $T_c$. In fact, a change in the ordering energy $\partial w_{ij}$ of 0.001 eV yields a reduction in $T_c$ of 10 °C. The critical temperature for $L1_2$ ordering in the tetrahedron approximation of Kikuchi's cluster variation method (CVM) is given as: $T_c = 0.96225|w_{ij}|/k$ [19–21]. For a non-polar interface, Benedek et al. [16] calculated a Cu–O bond length of 2 Å. In contrast, the calculation of the corresponding polar interface was 1.25 Å [16]. This substantial difference in interface separation between non-polar and polar interfaces will also change the interatomic potentials at the interface.

To obtain a deeper understanding of the influence of a polar interface on the ordering energy of $Cu_3Pd$ we have executed the following procedure. We are interested only in an estimate of the change of the critical

temperature of ordering as a function of the distance to the interface, i.e. we will concentrate on $\partial w_{ij}$ and not on the absolute value of $w_{ij}$. For the $Cu_3Pd$/MnO interface, there is an additional interaction across the interface that is not present along a homophase interface. According to classical electrostatics the negative charges in MnO at a distance $z_0$ from the interface induces a distribution of positive charge, which is confined to the interface with the metal. The distribution of positive charge acts as if a positive image charge exists at a site $z_0$ below the interface in the metal. Thus the charges in the ceramic are mirrored in a virtual 'mirror plane', which runs parallel to the interface, somewhere between the metal and the ceramic. Positive charges in the ceramic tend to form an excessive concentration of electrons on the other side of the mirror plane, while negatively charged ions create depleted regions in the electron sea. The electrostatic energy of the system is exactly half of the situation if the image charge were real point charges (due to correction of the self-energy [22]). The resulting potential $V$ due to the charge density induced on the metal surface can simply be formulated in term of classical electrostatics [23]. This description will break down at smaller distances because in real metals only charge distributions with a wavelength longer than the Fermi wavelength are permitted and rapid fluctuations in the charge distribution cannot occur. For the present analysis we take the discrete classical approach as a starting point [24]. In addition to the charge redistribution along the interface an interfacial dipole moment exists because of the atomic polarization of $Cu_3Pd$ by MnO. The polarization is crucial in stabilizing charged internal surfaces like {1 1 1} MnO. The energy change due to the dipole moment $\vec{P}$ can be written as

$$\partial E_{\mathrm{D},i} = \frac{1}{2}\sum_{i\neq j}\vec{P}(j)\cdot\vec{\nabla}V_{\mathrm{D}}(i,j), \tag{1}$$

where we take $V_{\mathrm{D}}(i,j)$ associated with the dipole as the Coulombic interaction between site $i$ and $j$. The factor 1/2 arises from the linearity of the medium response on the electric field. The interfacial dipole moment is described as $P = \sum_i z_i Q_i - \int z n(z)\,\mathrm{d}z$, where $n(z) = \int n(x,y,z)\,\mathrm{d}x\,\mathrm{d}y$ represents the electron clouds in the layer at $z$ and the discrete sum runs over the nuclear charge $Q_i$ at position $z_i$ [25–27]. $P$ was calculated from first-principles by making use of the spherical augmented plane wave (SAPW) method [28] and compared with the results for a simpler system of {1 1 1}$Mn_3O_4$/Pd calculated with the basic modules in the CASTEP [29] program. Details of the calculations examining also differences among various computational approaches [30,31] are presented elsewhere [32]. The excess interfacial dipole moment on Pd in the {1 1 1}MnO/$Cu_3Pd$ system with respect to {1 1 1}$Mn_3O_4$/Pd per Pd was found to be $4.8\times10^{-30}$ Cm. The dipole moment on Pd perpendicular to {1 1 1} in $Mn_3O_4$/Pd was calculated $-7.2\times10^{-30}$ Cm. Assuming only nearest neighbor interactions in the tetrahedron approximation of the CVM and that strongly ionic materials like MnO limit charge transfer but produces important polarization effect, $\partial E \approx \partial E_{\mathrm{D}}$ and $\partial E = 3\partial w_{ij}$ in $L1_2$ [33]. The change of the ordering energy $\partial w_{ij}$ as a function of the distance to the interface was obtained with Eq. (1) [34]. The results are displayed in Fig. 8 in terms of the suppression of the critical temperature for $L1_2$ ordering according to $\Delta T_{\mathrm{c}} = 0.96225|\partial w_{ij}|/k$ (tetrahedron approximation) [20]. Indeed, the polar interface affects the interactions in the metal but the range is too limited to affect the ordering behavior over 10 ML as was experimentally observed. For the sake of comparison, we have also calculated the dipole moment on Al as a function of the distance to a Al{1 1 1}/$Al_2O_3${0 0 0 1} interface. Again, the component of the dipole moment on Al perpendicular to the interface falls off very rapidly from the 1st to the 2nd {1 1 1} layer. The value of the dipole moment on Al perpendicular to the interface is found $-1\times10^{-30}$ Cm [35], i.e. of the same magnitude but smaller than on Pd in agreement with the fact that the atomic susceptibility of Pd is substantially larger than of Al [36]. In general we can conclude that the extension of the dipolar field in the metal due to these adhered ceramic materials is rather small, but in principle sufficient to disorder the first two MLs in the metal. The magnitude of the dipole moment of the various systems investigated is of equal order of magnitude and scales with the atomic susceptibility of the constituents. Now, to explain the experimentally observed extension of the disordered region over such a large distance, as 10 MLs besides the internal energy it is clear that also the (configurational) entropy has to be evaluated.

Support for this rather long-range effect of heterophase interfaces on the order (also for temperatures clearly below $T_{\mathrm{c}}$ and in particular for the parallel {1 1 1} interface in contrast to the {1 0 0} and {1 1 0} interfaces), comes from thermodynamic calculations including the

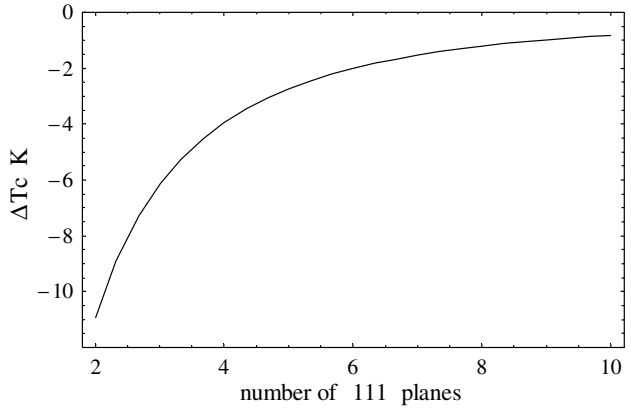


Fig. 8. Suppresion of the critical temperature for $L1_2$ ordering in the MnO/$Cu_3Pd$ system as a function of the distance (in units of the {1 1 1} interplaner distance in $Cu_3Pd$) to the polar {1 1 1} interface.

comfigurational entropy [37]. Here, the interface between $Al_3Li$ and Al is considered in most detail for a parallel (1 0 0) configuration, but also for the parallel (1 1 0) and (1 1 1) ones. The calculations are based on first principles to arrive at the interatomic potentials (up to second nearest neighbors) that are used as input in the CVM to obtain the composition profiles (including the degree of short and long-range order) perpendicular to the interface. It is shown that the calculated width of the interface boundary is a linear function of $T$ without any indication that it diverges when approaching $T_c$. This is in clear contrast to the wetting of APBs where the width of the disordered wetting layer is proportional to $\log(T - T_c)^{-1}$. The finite width originates from the fact that the $L1_2$ and fcc phases are related by a first- rather than by second-order phase transformations at $T_c$ and can be explained within the Landau–Ginzburg description of critical phenomena [38]. It should be noted that in the case of wetting the definition of the width is unambiguous, whereas in the former case it has a much more arbitrary basis. Nevertheless, referring to the width of the disordered layers as we observed in Figs. 3 and 5, the width of the diffuse region from order to complete disorder for the {1 0 0} $Al_3Li$–Al interface at 400 K (i.e. 280 K below $T_c$!) is already 12 {1 0 0} planes or 2.4 nm. In the light of these results it is not surprising that for the (more extreme) polar interfaces considered, cooled down after annealing 10 K below $T_c$, a region of 10 MLs is found where the order vanishes when approaching the interface. The conclusion of this analysis is that in the present system the dipolar contribution to the internal energy acts as an initiation of disordering along the MnO/$Cu_3Pd$ interface but that the extension of the disordered area into the intermetallic is determined by the entropic contribution. The configurational entropy is temperature dependent, the strength of which is affected by the specific crystallography. According to calculations in [37] $Al_3Li$/Al {1 0 0} interface boundaries do not contribute any excess configurational entropy until a certain temperature has been reached. These boundaries maintain sharp, whereas the {1 1 1} is predicted to have a disordered interface region even at lower temperature. Further, the dipole moment on Pd is also smaller in the case of a {1 0 0} MgO interface boundary [27] and consequently the effects on the ordering energy and $T_c$ will be smaller compared to the {1 1 1} interface. Together with a lower configurational entropy this will also contribute to a much smaller width of a {1 0 0} MnO/$Cu_3Pd$ interface and no extra compositional disorder will be introduced in accordance with our observations.

## 5. Conclusions

Using HRTEM, we show that the $L1_2$ ordering at polar {1 1 1} $Cu_3Pd$–MnO interfaces gradually disappears when annealed at a temperature 10 K below $T_c$. This effect is observed both for viewing in the ⟨1 1 0⟩ and ⟨1 1 2⟩ projection. On the other hand, non-polar {0 0 2} $Cu_3Pd$–$Mn_3O_4$ interfaces did not exhibit an influence on the $L1_2$ order even close to the interface and near $T_c$. The disordering effect we observed has a completely different physical origin and behavior than the wetting of APBs very close to $T_c$. The conclusion of our analysis is that the dipolar contribution to the internal energy acts as an initiation of disordering along the MnO/$Cu_3Pd$ interface but that the configurational entropy determines the extension of the disordered area.

## Acknowledgements

This work is part of the research program of the Foundation for Fundamental Research on Matter (Utrecht, The Netherlands) and has been made possible by financial support form the Netherlands Organization for Research (NWO, The Hague) and the Netherlands Institute for Metals Research. Thanks are due to the Max-Planck Institute für Metallforschung MPI- Stuttgart (Dr. F. Phillip) giving access and assistance to the JEOL ARM 1250 transmission electron microscope.

## References

[1] Westbrook JH, Fleischer RL, editors. Intermetallic compounds, vol. 3. New York: Wiley; 2000.
[2] Broddin D, Tendeloo G, van Landuyt J, Amelinckx S. Phil Mag A 1986;54:395.
[3] Broddin D, van Tendeloo G, van Landuyt J, Amelinckx S. Phil Mag B 1988;57:31.
[4] Guymont M, Gratias D. Phys Status Solidi A 1976;36:318.
[5] Rhines FN, Grobe AH. Trans AIME 1942;147:318.
[6] Tichelaar FD, Schapink FW, Li X. Phil Mag A 1992;65:913.
[7] Kooi BJ, Wouters O, De Hosson JTM. Acta Mater 2002;50:223.
[8] Mogck S, Kooi BJ, De Hosson JTM. Phil Mag 2003;83:727.
[9] Mogck S, Kooi BJ, De Hosson JTM. Interface Sci 2004;12:39.
[10] Kooi BJ, De Hosson JTM. Acta Mater 1998;46:1909.
[11] Kilaas R. In: Proceedings of the 49th annual EMSA meeting; 1991. p. 528.
[12] Baker H. Handbook. Alloy phase diagrams, vol. 3. Materials Park, OH: American Society for Metals; 1992.
[13] Mader W. Z Metallkd 1992;83:7.
[14] Backhaus-Ricoult M. Acta Mater 2001;48:4365.
[15] Carlsson JM. Elect Comp Mater Sci 2001;22:24.
[16] Benedek B, Minkoff M, Yang LH. Phys Rev B 1996;54:7697.
[17] Heine V. Phys Rev A 1965;138:1689.
[18] Muller D, Shashkov DA, Benedek R, Yang LH, Silcox J, Seidman DN. Phys Rev Lett 1998;80:4741.
[19] Kikuchi R. Phys Rev 1951;81:988.
[20] De Fontaine D. In: Ehrenreich H, Seitz F, Turnbull D, editors. Solid state physics, vol. 34; 1979. p. 73.
[21] de Rooy A, van Royen EW, Bronsveld PM, De Hosson JTM. Acta Metall 1980;28:1315.
[22] Finnis M. Interatomic forces in condensed matter. Oxford: Oxford University Press; 2003. p. 82.
[23] Duffy DM, Harding JH, Stoneham AM. Acta metall mater 1992;40:S11.

[24] Finnis MW. Acta metall mater 1992;40S:S25.
[25] Bader RFW. Chem Rev 1991;91:893.
[26] Ganiakowski J, Noguera C. Phys Rev 1991;60:16120.
[27] Ganiakowski J, Noguera C. Interface Sci 2004;12:93.
[28] Slater J. Adv Quantum Chem 1973;6:1.
[29] Available from: http://www.accelrys.com/cerius2/castep.html.
[30] Vanderbilt D. Phys Rev B 1990;41:7892.
[31] Payne MC, Teter MP, Allan DC, Arias TA, Joannopoulos JD. Rev Mod Phys 1992;64:1045.
[32] Mogck S, Kooi BJ, De Hosson JTM, Finnis M. Phys. Rev. B [to be published].
[33] De Hosson JTM. In: Lee JK, editor. Interatomic potentials and crystalline defects, TMS-AIME; 1981. p. 3–32.
[34] Duffy DM, Harding JH, Stoneham AM. Acta metall mater 1992;40:S11.
[35] Haarsma H, De Hosson JTM. Phil. Mag. [submitted]. Available from: http://www.ub.rug.nl/eldoc/dis/science/h.s.d.haarsma/.
[36] American institute of physics handbook. New York: McGraw-Hill Book Company; 1972. p. 5–224.
[37] Sluiter M, Kawazoe Y. Phys Rev B 1996;54:10381.
[38] Ducastelle F. In: Moran Lopez JL, editor. Structure and phase stability of alloys. New York: Plenum Press; 1992. p. 231.